NUCLEAR SCIENCE AND ENGINEERING: 99, 299-312 (1988)

Study on Coolant Void Reactivity of Pressure-Tube-Type Heavy Water Lattice by the Substitution Method

Yasuki Kowata and Nobuo Fukumura

Power Reactor and Nuclear Fuel Development Corporation, Oarai Engineering Center
Oarai-machi, Ibaraki-ken, Japan

Received July 14, 1987
Accepted January 29, 1988

Abstract—*Using the substitution method combined with the pulsed neutron technique, coolant void reactivities of PuO_2-UO_2 fuel lattices in pressure-tube-type heavy water reactors have been determined as functions of PuO_2 enrichment in PuO_2-UO_2 (0.54 and 0.87 wt%), fissile content of plutonium (91 and 75% fissile plutonium), lattice pitch (V_m/V_f: 7.4 and 9.9), and coolant void fraction (0, 30, 70, 87, and 100%). The reference loading of 1.2 wt% enriched UO_2 clusters was progressively replaced by PuO_2-UO_2 test clusters.*

The void reactivities were obtained from Simmons and King's formula in which correction was made for a change of the prompt generation time. As decay constants can be maintained invariable due to substitution, buckling differences were analyzed by the first-order perturbation method, on the assumption that lattices are homogeneous and no difference in diffusion coefficients exists between the two lattices.

Void reactivities of test lattices were determined with an accuracy of ~10% when the minimum number of test fuel clusters was ~5% of the total. The void reactivity shifted farther to the negative side as the proportion of fissile plutonium was increasingly in the PuO_2-UO_2 fuel of the same enrichment of plutonium.

I. INTRODUCTION

Since boiling light-water-cooled, pressure-tube-type heavy water reactors (HWRs) have a good neutron economy, the flexibility of selecting fuel is greater compared to that for light water reactors.[1] The moderator is spatially isolated from fuel clusters, and the temperature is kept much lower than the saturation temperature. Thermalization of neutrons is sufficiently carried out in the moderator, but the spatial distribution of void fraction arises in light water coolant flowing in pressure tubes. Coolant void reactivity became an important factor from the nuclear safety viewpoint after the reactivity accident at Chernobyl Unit 4.

The HWR core, being developed in Japan,[2] has been designed so that plutonium-uranium mixed-oxide (PuO_2-UO_2 MOX) fuel can be used over the whole core. Although MOX fuel has the effect of shifting coolant void reactivity to the negative side as compared with the case of using uranium fuel, the reactivity changes largely according to the form and composition of the fuel and due to the change of the isotope ratio of plutonium accompanying burnup. Therefore, in a core design that aims to achieve higher burnup compared with the prototype HWR FUGEN, it is necessary to understand the dependence of the coolant void reactivity of MOX fuel lattices on fuel composition and lattice pitch, and the phenomenon of reactor physics.

To accurately determine the coolant void reactivity of various kinds of MOX fuel lattices, a critical experiment using a one-region core is performed; however, to realize the critical condition by this method, generally a large number of each of the fuel clusters must be prepared. Consequently, MOX fuel lattice information must be obtained from a critical experiment using a small number of the MOX fuel clusters; therefore, the substitution method is generally employed.[3-11] Substitution method techniques have mainly been applied to determine material buckling.[12,13] To determine material buckling, the few-group diffusion theory combined with homogenization of regions[3-5] is generally adopted. Persson[10,11] has used the analysis

based on the first-order perturbation theory by successfully introducing a transition region between a reference and a test lattice. For determining the material buckling of the HWR lattice using cluster-type fuel, Shiba[13] treated the change of critical buckling due to substitution as the change of an eigenvalue using the second-order perturbation theory.

So far, material buckling has been determined by taking the perturbation in the analysis of experimental data as far as possible. The substitution method, however, has not been used to determine physical characteristics such as reactivity in a test lattice. If the reactivity due to the change of the coolant void fraction is measured by the pulsed-neutron method, for determining the coolant void reactivity in a test lattice by the substitution method, material bucklings in a test lattice and also the response to the pulsed neutrons must be taken together in the analysis.

In this study, we show that the relationship between the prompt neutron decay constant and the change in buckling due to substitution can be analyzed by using the first-order perturbation theory and that the coolant void reactivity of a test lattice can be determined. We consider the following features for HWR lattices:

1. The mutual intervals of the fuel clusters are widely spaced.
2. The moderator-to-fuel volume ratio is sufficiently large.
3. At the boundary of adjacent lattices, the neutron spectra in heavy water are not largely affected by types of fuel and therefore soften sufficiently.

By applying this analysis method to the substitution measurement on the HWR lattice using a 28 fuel rod cluster, the difference of coolant void reactivity due to uranium or plutonium and the lattice pitch is clarified.

II. EXPERIMENTAL PROCEDURE

The coolant void reactivity of the HWR lattice using MOX fuel was determined by the substitution method combined with the pulsed neutron technique in a deuterium critical assembly (DCA). As shown in Fig. 1, the DCA core is contained in a 3-m-i.d., 3-m-high aluminum tank with a 1-cm-thick wall. The fuel clusters in the core are arranged in a 22.5-cm square lattice or 25.0-cm pitch so that the reflector does not

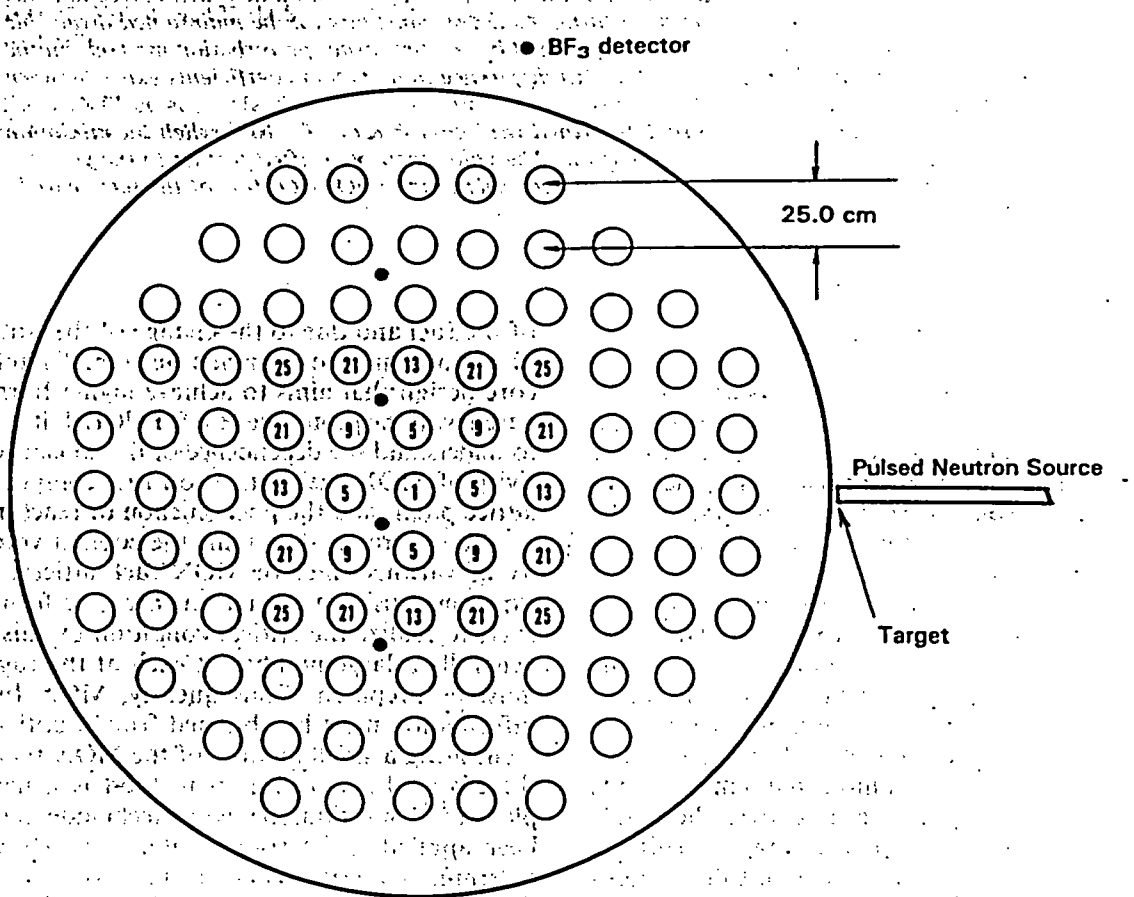

Fig. 1. Loading patterns of test fuel clusters whose positions are represented by numbered circles.

attach. The fuel clusters used for the experiment have an effective length of 2 m. A 28 fuel rod cluster arranged in 3 layers of concentric circles was used as shown in Fig. 2. These fuel rod clusters are isolated from the heavy water moderator by pressure tubes, air gaps, and calandria tubes.

The criticality is adjusted by changing the moderator level, which is measured with a servomanometer in a communicating tube with a ±0.1-mm accuracy. The heavy water is 99.45 mol% pure and is nonpoisonous. During the substitution measurement, the temperature of the moderator changed by about ±1.0°C. However, the uncertainty of coolant void reactivity due to this temperature change is negligibly small.

In the pressure tubes, light water, air, or the proper mixtures of heavy water and light water were used as coolant. The level of coolant in the pressure tubes was adjusted to nearly equal the level of the moderator. To simulate coolant void, these mixtures were adjusted so that the slowing down powers equaled that of the coolants of 30, 70, and 87% void fractions, respectively. A small quantity of boric acid was added for adjusting the absorption cross section in a thermal energy region as shown in Table I. A comparison of the cross sections of the simulated coolants and the coolant having actual void fraction is shown in Table II.

In the substitution measurement, lattices fueled with 1.2 wt% enriched uranium oxide (1.2 UO_2) were used for reference. The central part of the reference core was progressively substituted with test clusters of PuO_2-UO_2 fuel. The various test regions in the measurement comprised 1, 5, 9, 13, 21, and 25 fuel clusters. Substitution was carried out so as to be fourfold rotation symmetry around the core axis as shown in Fig. 1. In respective partially substituted cores, the coolant void reactivity was measured by the pulsed neutron method as a function of the number of test fuel clusters. The composition of the fuel clusters investigated is given in Table III. The proportion of fissile plutonium to total plutonium was ~91% standard grade (S) or 74% reactor grade (R). The proportion of fissile content in the 0.54(S) PuO_2-UO_2 fuel was equal to that of the 1.2 UO_2 fuel.

The prompt neutron decay constant was measured as a function of axial buckling in the pulsed neutron experiment. The pulsed neutrons generated by the D(T,α)n reaction using a Cockcroft-Walton-type accelerator were injected into the core, and the attenuation of neutron density was measured by four 0.5-in.-diam BF_3 detectors as shown in Fig. 1. The detector

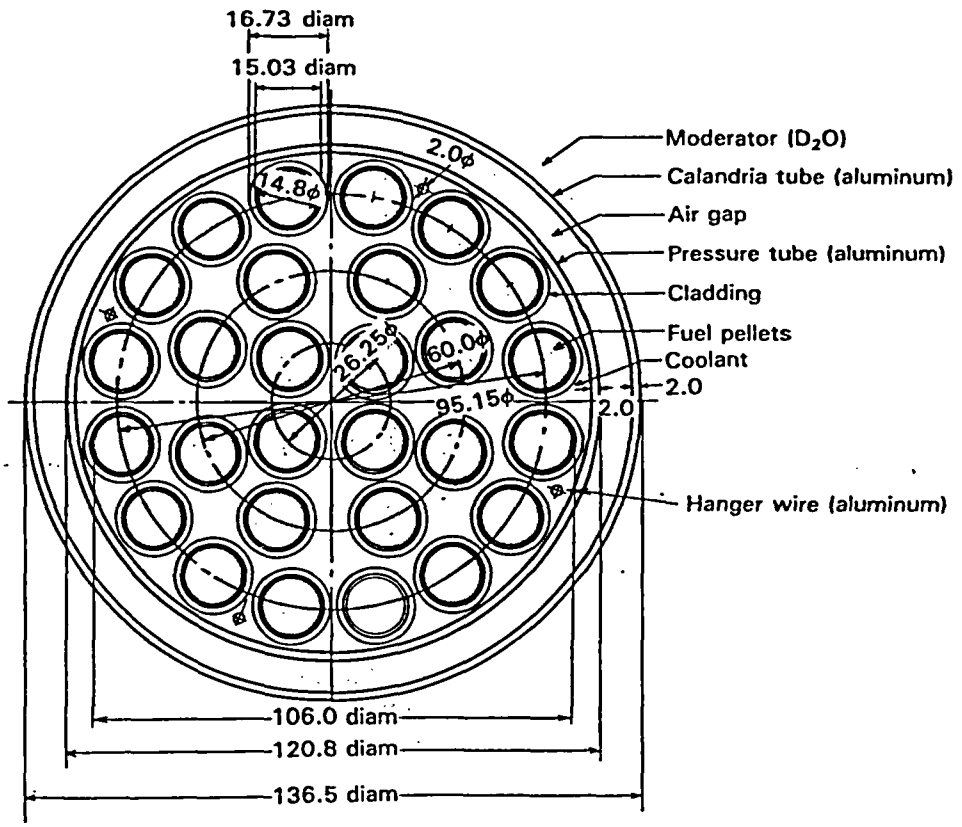

Fig. 2. Cross-sectional view of the fuel assembly. Dimensions are given in millimetres.

TABLE I

Ingredient of Coolants Simulating Void

Simulated Void Fraction (%)	Content of Nuclide in Coolants (wt%)					Density (g/cm³)
	Hydrogen	Deuterium	Oxygen	Boron (Natural)	Nitrogen	
0	11.190	---	88.810	---	---	0.9978
30	7.069	7.405	85.523	0.00161	---	1.0348
70	2.023	16.474	81.500	0.00376	---	1.0840
87	0.050	20.022	79.928	---	---	1.1045
100	---	---	23.520	---	76.480	0.0012

TABLE II

Ratios of Two-Group Cross Sections Between Simulated and Actually Voided Coolants

Simulated Void Fraction (%)	Ratios of Simulated to Actually Voided Coolants				
	Epithermal		Thermal		
	$\xi\Sigma_s$	Σ_{tr}	Σ_a	Σ_s	Σ_{tr}
30	1.000	1.163	1.000	1.008	1.020
70	0.999	1.890	1.000	1.004	1.110
87	1.000	1.616	0.871	1.003	1.048

heights were adjusted so that they were nearly at the midpoint of the moderator level. The count rate $n(t)$ of respective detectors was fitted to the function $n(t) = A\exp(-\alpha t) + C$ by the least-squares method, and the prompt neutron decay constant (α) was determined. The final value of α was obtained by averaging four α, independent of the fitting starting time difference. The statistical error of α was within 2%.

The moderator level was converted to axial buckling. To determine effective axial extrapolation distances including the reflector saving due to the upper and lower structures, the reactor flux profile measurements using copper activation were taken in reference and partially substituted cores. The axial flux distributions measured at the center of a fuel cluster and moderator were least-squares fitted to a cosine function to evaluate effective core heights. The least-squares fitting was undertaken by successively dropping data near the core boundaries until fixed values of the effective core height were obtained. The fixed values showed no meaningful dependence on the transversal location in the unit cell, fuel kind, and lattice pitch as long as there was little change in the coolant void fraction. Effective axial extrapolation distances were determined from these fixed values as 11.3 ± 0.6 or 10.2 ± 0.6 cm depending on whether the coolant void fraction was 100% (air) or some other value.

The radial flux distribution measured at the centers of fuel clusters in the reference core was least-squares fitted to the J_0 function to evaluate the effective core radius that was needed for determining statistical weights of substituted regions. The effective core radii obtained are shown in Table IV.

III. PRINCIPLE OF DATA ANALYSIS

III.A. Buckling in a Fully Substituted Core

When the region occupying a test lattice changes due to substitution, radial neutron flux distribution is distorted. However, the composition in the axial direction of the core is uniform. Accordingly, if the size of a substituted region is determined, axial neutron flux distribution always becomes the cosine distribution determined by the geometric buckling. Then, the prompt neutron decay constant α becomes a function of only axial buckling B_z^2 for respective partially substituted cores. Here, by fitting the data of α and B_z^2 into the equation[14]

$$\alpha(B_z^2) = \alpha_c + b(B_z^2 - B_{zc}^2) + c(B_z^2 - B_{zc}^2)^2 \quad (1)$$

by the least-squares method for every substituted core, the prompt neutron decay constant at critical α_c and the first- and second-order differential coefficients b and c were determined. In Eq. (1), B_{zc}^2 is the axial critical buckling.

By applying the first-order perturbation theory to Eq. (1) for every partially substituted core, we determined α_c, b, and c in a fully substituted core (test lattice). For simplification, we assumed that (a) neutron energy groups are two groups, (b) every lattice is homogeneous, and (c) diffusion approximation can be applied.

The prompt neutron flux $\Phi(r,t)$ in the reference core (reference lattice) having B_z^2 just after injecting pulsed neutrons follows the equation

TABLE III

Fuel Composition Used in Experiments on 28 Fuel Rod Clusters

Kind	Fuel Type	Nominal Enrichment (wt%)	Ratio of Plutonium Fissile (wt%)	Cladding Material	Content of Nuclide in Pellets (wt%)						
					^{238}Pu	^{239}Pu	^{240}Pu	^{241}Pu	^{242}Pu	^{235}U	^{238}U
Test	0.54(S) PuO_2-UO_2	0.54 (PuO_2)	91	Zircaloy-2	1.0×10^{-4}	0.430	0.041	4.3×10^{-3}	3.0×10^{-4}	0.621	86.782
	0.87(S) PuO_2-UO_2	0.87 (PuO_2)	91	Zircaloy-2	1.4×10^{-4}	0.685	0.065	6.9×10^{-3}	5.1×10^{-4}	0.619	86.503
	0.87(R) PuO_2-UO_2	0.87 (PuO_2)	74	Zircaloy-2	6.4×10^{-3}	0.495	0.166	7.2×10^{-2}	2.3×10^{-2}	0.619	86.493
Reference	1.2 UO_2	1.2 (^{235}U)	---	Al	---	---	---	---	---	1.057	86.793

TABLE IV

Effective Core Radius of Reference Core

Lattice Pitch (cm)	R^a (cm)	Void Fraction (%)	B_r^2 (m^{-2})	Effective Core Radius, R_0 (cm)
22.5	139.6	0, 30, 70, 87	2.47 ± 0.04	153.0 ± 1.0
		100	2.36 ± 0.04	156.5 ± 1.0
25.0	138.9	0	2.45 ± 0.02	153.8 ± 1.0
		100	2.31 ± 0.02	158.2 ± 1.0

[a]Here, R = equivalent core radius [$= (nP^2/\pi)^{1/2}$] where n = total number of unit cell, and P = lattice pitch.

$$V^{-1}\frac{\partial \Phi(r,t)}{\partial t} = \mathbf{L}\Phi(r,t) \ , \tag{2}$$

where $\Phi(r,t)$ and V^{-1} are the neutron flux and neutron velocity reciprocal, respectively, and an operator $\mathbf{L}$ is shown as

$$\mathbf{L} = \begin{bmatrix} D_{1r}\nabla^2 - D_{1z}B_z^2 - \Sigma_1 & (1-\beta_{eff})\nu\Sigma_{f2} \\ p\Sigma_s & D_{2r}\nabla^2 - D_{2z}B_z^2 - \Sigma_{a2} \end{bmatrix} . \tag{3}$$

Subscripts 1 and 2 show the fast and thermal energy groups, respectively, and other symbols have their conventional meanings. Here, $\Phi(r,t)$ is postulated as

$$\Phi(r,t) = \Phi(r)\cdot\exp(-\alpha t) \ . \tag{4}$$

Then, Eq. (2) and its adjoint equation become

$$-\alpha V^{-1}\Phi(r) = \mathbf{L}\Phi(r) \tag{5}$$

and

$$-\alpha V^{-1}\Phi^\dagger(r) = \mathbf{L}^\dagger\Phi^\dagger(r) \ , \tag{6}$$

where $\Phi^\dagger(r)$ and $\mathbf{L}^\dagger$ are the adjoint neutron flux of $\Phi(r)$ and adjoint operator of $\mathbf{L}$, respectively.

When part of the reference lattice is substituted with a test lattice to be investigated, the original core is perturbed. The perturbation along the axial direction of the core in a substituted region is uniform; therefore, α can be maintained invariably even if substitution is done by adjusting B_z^2 by δB_z^2. Since the content of fissile substances in the fuel was low, it was clarified by the lattice calculation that the change of the average neutron velocity due to substitution was <1%. From this result, the behavior of neutron flux in a partially substituted core conforms to

$$-\alpha V^{-1}\Phi^*(r) = [\mathbf{L}' + W(r)\delta\mathbf{L}']\Phi^*(r) \ , \tag{7}$$

where

$\Phi^*(r)$ = prompt neutron flux of a perturbed core

$\mathbf{L}'$ = operator being replaced by B_z^2 with $(B_z^2 + \delta B_z^2)$ in Eq. (3)

$\delta\mathbf{L}'$ = operator representing the perturbation of $\mathbf{L}'$.

The value $W(r)$ is defined as

$$W(r) = \begin{cases} 1 & \text{in a substituted region} \\ 0 & \text{in a nonsubstituted region} \end{cases} .$$

The infinitesimal quantity of second order $(\delta D \cdot \delta B_z^2)$ is as small as can be neglected. Therefore, neglecting this quantity, Eq. (7) is rewritten as

$$-\alpha V^{-1}\Phi^*(r) \approx [\mathbf{L} - \delta B_z^2 \cdot \mathbf{D}_z + W(r)(\delta\mathbf{L}_1' + \delta\mathbf{L}_2')]\Phi^*(r) , \quad (8)$$

where $\mathbf{D}_z$, $\delta\mathbf{L}_1'$, and $\delta\mathbf{L}_2'$ are expressed as

$$\mathbf{D}_z = \begin{bmatrix} D_{1z} & 0 \\ 0 & D_{2z} \end{bmatrix} , \quad (9a)$$

$$\delta\mathbf{L}_1' = \begin{bmatrix} -\delta D_{1z} \cdot B_z^2 - \delta\Sigma_1 & \delta(1-\beta_{eff})\nu\Sigma_{f2} \\ 0 & -\delta D_{2z} \cdot B_z^2 - \delta\Sigma_{a2} \end{bmatrix} , \quad (9b)$$

and

$$\delta\mathbf{L}_2' = \begin{bmatrix} -\nabla\delta D_{1r} \cdot \nabla & 0 \\ 0 & -\nabla\delta D_{2r} \cdot \nabla \end{bmatrix} . \quad (9c)$$

When both sides of Eqs. (6) and (8) are multiplied by $\Phi^*(r)$ and $\Phi^\dagger(r)$ from the left, respectively, and then the inner product is subtracted from the other one, we get

$$-\delta B_z^2 \langle \Phi^\dagger(r), \mathbf{D}_z\Phi^*(r)\rangle + \langle \Phi^\dagger(r), W(r)(\delta\mathbf{L}_1' + \delta\mathbf{L}_2')\Phi^*(r)\rangle = 0 , \quad (10)$$

where $\langle\ \rangle$ represents the inner product. Accordingly, when α is invariable in a partially substituted core, the change δB_z^2 from B_z^2 becomes

$$\delta B_z^2 = \frac{\langle \Phi^\dagger(r), W(r)\delta\mathbf{L}_1'\Phi^*(r)\rangle - \langle W(r)\cdot\delta\mathbf{D}_r|\nabla\Phi^\dagger(r)\cdot\nabla\Phi^*(r)|\rangle}{\langle \Phi^\dagger(r), \mathbf{D}_z\Phi^*(r)\rangle} , \quad (11)$$

where

$$\delta\mathbf{D}_r = \begin{bmatrix} \delta D_{r1} & 0 \\ 0 & \delta D_{r2} \end{bmatrix} .$$

As mentioned in Sec. II, the axial extrapolation distance related to the diffusion coefficient does not depend on fuel composition. Consequently, $\delta\mathbf{D}_r$ due to substitution is considered to be as small as can be neglected. The second term on the right side of Eq. (11) can be regarded as sufficiently small as compared with the first term. Then Eq. (11) can be approximated as

$$\delta B_z^2 \approx \frac{\langle \Phi^\dagger(r), W(r)\delta\mathbf{L}_1'\Phi^*(r)\rangle}{\langle \Phi^\dagger(r), \mathbf{D}_z\Phi^*(r)\rangle} . \quad (12)$$

The nuclear coupling between lattices is weak in an HWR; therefore, $\Phi^*(r)$ in a partially substituted core can be considered spatially proportional to a shape function $\phi(r)$. Then, variables can be separated in each region, and $\Phi^*(r)$ is expressed by

$$\Phi^*(r) = \begin{cases} \begin{bmatrix} \psi_{1s}^* \\ \psi_{2s}^* \end{bmatrix}\phi(r) & \text{in a test lattice region} \\ \begin{bmatrix} \psi_{1r}^* \\ \psi_{2r}^* \end{bmatrix}\phi(r) & \text{in a reference lattice region} \end{cases} , \quad (13)$$

where ψ_{1s}^*, ψ_{2s}^*, ψ_{1r}^*, and ψ_{2r}^* are the constant values representing neutron spectra, respectively. The $\Phi^\dagger(r)$ value of a reference core is also proportional to the shape function $\phi_0(r)$; therefore, $\Phi^\dagger(r)$ is shown by

$$\Phi^\dagger(r) = \begin{bmatrix} \psi_1^\dagger \\ \psi_2^\dagger \end{bmatrix}\phi_0(r) . \quad (14)$$

When Eq. (12) is rewritten by using Eqs. (13) and (14), δB_z^2 results in

$$\delta B_z^2 \approx A \cdot W_0 , \quad (15)$$

where the proportional constant A and the statistical weight[14] W_0 are expressed as

$$A = \frac{\delta(1-\beta_{eff})\nu\Sigma_{f2}\psi_1^\dagger\psi_{2s}^* - \delta\Sigma_1\psi_1^\dagger\psi_{1s}^* + \delta\Sigma_{a2}\psi_2^\dagger\psi_{2s}^*}{D_{1z}(\psi_{1s}^* + \psi_{1r}^*)\psi_1^\dagger + D_{2z}(\psi_{2s}^* + \psi_{2r}^*)\psi_2^\dagger} . \quad (16)$$

and

$$W_0 = \frac{\langle \phi(r), W(r)\phi_0(r) \rangle}{\langle \phi(r), \phi_0(r) \rangle} \quad . \tag{17}$$

In a fully substituted core (test lattice), W_0 becomes 1.0; therefore, δB_z^2 is determined by the gradient A of Eq. (15). Similarly, critical buckling B_{zc}^2 in a fully substituted core is determined. Then, the relation between α and B_z^2 in a fully substituted core is determined.

III.B. Statistical Weight in a Substituted Core

As shown in Sec. I, for determining the physical characteristics of test lattices by using the first-order perturbation method, the accuracy of W_0 is important. In this study, an attempt was made to determine W_0 analytically in a partially substituted core.

Since the substitution was done with fourfold rotation symmetry, the substituted region is regarded as the equivalent cylindrical form. In this case, W_0 can be obtained from the neutron flux distribution in a concentric cylindrical form two-region core. Equation (17) is expressed by

$$W_0 = \frac{\int_0^{R_1} \phi_0(r)\phi(r) r\,dr}{\int_0^{R} \phi_0(r)\phi(r) r\,dr} \quad , \tag{18}$$

where R and R_1 are the equivalent radii of a core and a substituted region, respectively.

Let us assume that the neutron flux distribution $\phi(r,z)$ in a partially substituted core is expressed by the Helmholtz equation, such that

$$\nabla^2 \phi_i(r,z) + B_{m,i}^2 \phi_i(r,z) = 0 \quad , \quad i = 1,2 \quad , \tag{19}$$

where $B_{m,i}^2$ is the material buckling in a lattice of i'th region: a test lattice ($i = 1$) and a reference lattice ($i = 2$).

When $\phi_i(r,z)$ is defined as

$$\phi_i(r,z) = \phi_i(r)\cos B_z z \quad , \tag{20}$$

Eq. (19) becomes

$$\nabla_r^2 \phi_i(r) + (B_{m,i}^2 - B_z^2)\phi_i(r) = 0 \quad , \tag{21}$$

where

$$\nabla_r^2 = \frac{1}{r}\frac{\partial}{\partial r} r \frac{\partial}{\partial r} \quad .$$

The general solution of Eq. (21) becomes

$$\phi_i(r) = A_i J_0(\lambda_i r) + B_i Y_0(\lambda_i r) \quad , \tag{22}$$

with

$$\lambda_i = (B_{m,i}^2 - B_z^2)^{1/2} \quad ,$$

where

A_i, B_i = constants

J_0, Y_0 = Bessel functions of zero order.

When Eq. (22) is solved under the general boundary condition, the radial flux distribution in a partially substituted core $\phi(r)$ is given by

$$\phi(r) = \begin{cases} A_1 J_0(\lambda_1 r) \quad , & 0 \le r \le R_1 \quad , \\ A_1 \eta \left[J_0(\lambda_2 r) - \dfrac{J_0(\lambda_2 R)}{Y_0(\lambda_2 R)} Y_0(\lambda_2 r) \right] \quad , & R_1 \le r \le R_0 \quad , \end{cases} \tag{23}$$

where R_0 is the effective radius of a core, and η is expressed by

$$\eta = \frac{D_1 \lambda_1 J_1(\lambda_1 R_1) - J_0(\lambda_1 R_1)}{[D_2 \lambda_2 J_1(\lambda_2 R_1) - J_0(\lambda_2 R_1)] - \dfrac{J_0(\lambda_2 R)}{Y_0(\lambda_2 R)} [D_2 \lambda_2 Y_1(\lambda_2 R_1) - Y_0(\lambda_2 R_1)]} \quad , \tag{24}$$

where

D_1, D_2 = diffusion coefficients of a test lattice and a reference lattice, respectively

J_1, Y_1 = Bessel functions of order n.

Next, we attempt to determine W_0 in a partially substituted core. Corresponding to Eq. (18), W_0 is expressed by

$$W_0 = 2\pi \int_0^{R_1} \phi_0(r)\phi(r) r\,dr \quad . \tag{25}$$

Since $\phi_0(r)$ is the radial flux distribution in the reference core, it is shown by using a constant A_0 as

$$\phi_0(r) = A_0 J_0(\lambda_0 r) \quad , \tag{26}$$

where $\lambda_0 = 2.405/R_0$. When the range of integration is from $r = 0$ to $r = R$ in Eq. (25), the normalization is $W_0 = 1.0$. The W_0 value is determined by using Eqs. (23) and (26):

$$W_0 = \epsilon \frac{R_1}{(\lambda_0^2 - \lambda_1^2)} [\lambda_0 J_1(\lambda_0 R_1) J_0(\lambda_1 R_1) - \lambda_1 J_1(\lambda_1 R_1) J_0(\lambda_0 R_1)] \quad , \tag{27}$$

where ϵ is the normalization factor.

The value W_0 was analytically determined when the size of a substituted region and $B^2_{m,1}$ were determined. As the material buckling of a test lattice B^2_m $(=B^2_{m,1})$ depends on W_0 as shown in Eq. (15), W_0 and B^2_m were determined by an iterative procedure. An example of the relation between the number of test fuel clusters and W_0 is shown in Fig. 3.

III.C. Derivation of Coolant Void Reactivity

Coolant void reactivity $\rho_{v\to v'}$ (dollar) is the reactivity that arises when the coolant void fraction in pressure tubes is changed from V% to V'% $(V<V')$. The value $\rho_{v\to v'}$ was determined by following Simmons and King's formula[15]:

$$\frac{\rho_{v\to v'}}{\beta_{eff}} = 1 - \frac{\alpha(B^2_{zv})}{\alpha_c} \cdot \frac{\Lambda(B^2_{zv})}{\Lambda_c} , \qquad (28)$$

where

α_c, Λ_c = decay constant and generation time of prompt neutron in a critical core of void fraction V'%, respectively

B^2_{zv} = critical axial buckling in a core of void fraction V%.

In Eq. (28), we corrected for the change of the prompt neutron generation time.[16]

The correction term Λ/Λ_c for prompt neutron generation time is expressed by

$$\frac{\Lambda(B^2_{zv})}{\Lambda_c} = \frac{l(B^2_{zv})}{l_c}\left[1 - \beta_{eff}(\rho_{v\to v'}/\beta_{eff})\right] . \qquad (29)$$

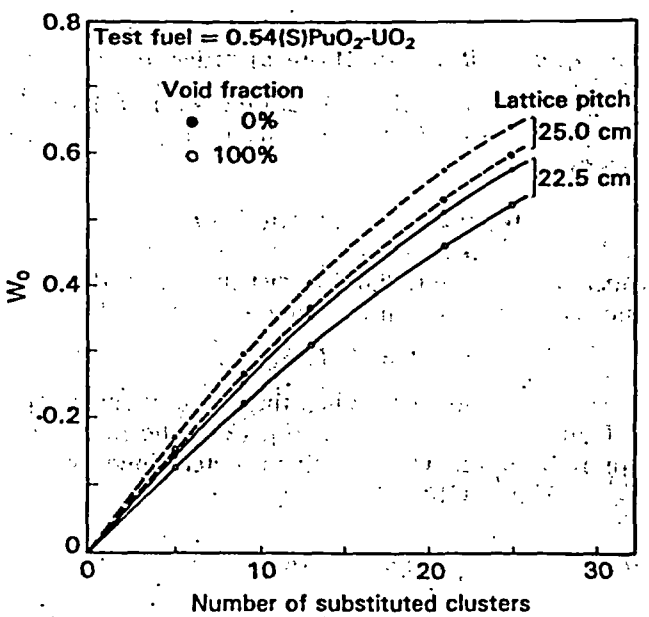

Fig. 3. Relation between number of substituted clusters and statistical weight.

According to the simple few-group core calculation, the value of Λ/Λ_c was estimated as <7% in the range of this experiment. Therefore, Eq. (29) can be approximated as

$$\frac{\Lambda(B^2_{zv})}{\Lambda_c} \approx 1 - \beta_{eff}(\rho_{v\to v'}/\beta_{eff}) + \frac{1}{l_c}\frac{\partial l}{\partial B^2_z}(B^2_{zv} - B^2_{zc}) , \qquad (30)$$

where

β_{eff} = effective delayed neutron fraction in a core after reactivity was imposed

l_c = lifetime of prompt neutrons at critical

$\partial l/\partial B^2_z$ = differential coefficient of the lifetime in relation to B^2_z.

Using Eqs. (28) and (30), $\rho_{v\to v'}$ (dollar) after the correction was determined by the iterative calculation.

Since the amount of correction of the generation time was small, the values used for this correction were obtained by the few-group lattice calculation code[17] METHUSELAH and the diffusion calculation code[18] CITATION. The evaluation of accuracy of the METHUSELAH code was carried out with the DCA and has been used for the nuclear design of the Japanese prototype HWR.

IV. RESULTS AND DISCUSSION

IV.A. Void Reactivity by the Substitution Method

The typical results of the relation between α and B^2_z are shown in Fig. 4. In this figure, the continuous line is obtained by fitting the values of α and B^2_z to Eq. (1) by the least-squares method. The prompt neutron decay constant α_c was obtained by extrapolating α up to the critical buckling B^2_{zc}. The coefficient c was <2% as compared with the coefficient b and was sufficiently small. The errors of α_c and b by least-squares fitting were both on the average of 2%.

An example of the experimental results representing the dependence of δB^2_z on W_0 at critical and subcritical are shown in Figs. 5 and 6, respectively. Continuous lines show the results of least-squares fitting by Eq. (15). As clearly seen in these figures, the propriety of Eq. (15) was sufficiently confirmed. The critical axial buckling B^2_{zc} of each lattice is shown in Table V together with B^2_m. In the DCA core, the component of B^2_z in relation to B^2_m was >70%. The B^2_m value of the test lattice was determined with an accuracy of 3% at maximum, and B^2_m decreases when the coolant void fraction is increased. On the other hand, B^2_m decreases or increases when the lattice pitch is increased. It is clear from Table V that B^2_m of 0.54(S) PuO_2-UO_2 fuel increased by ~40% at 0% void fraction and increased by ~20% at 100% void

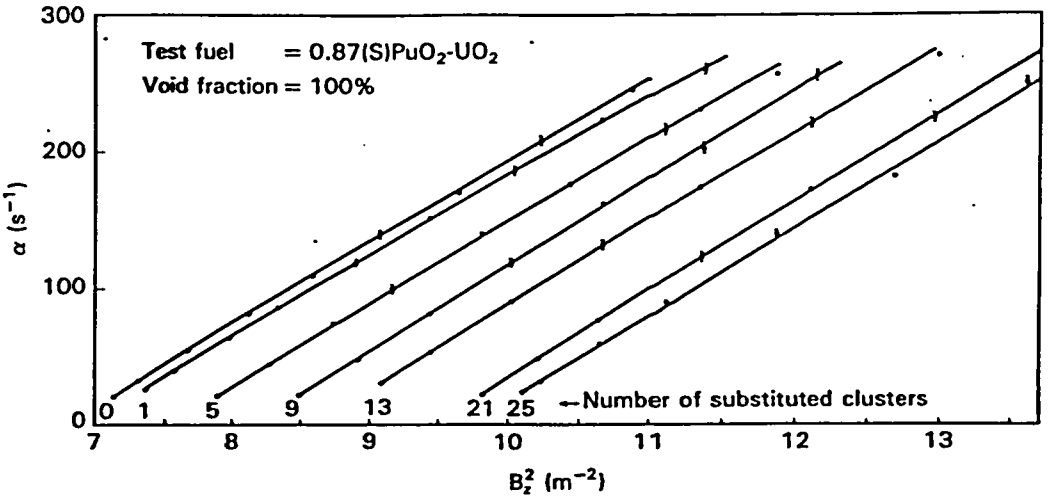

Fig. 4. Prompt decay constant as a function of axial buckling.

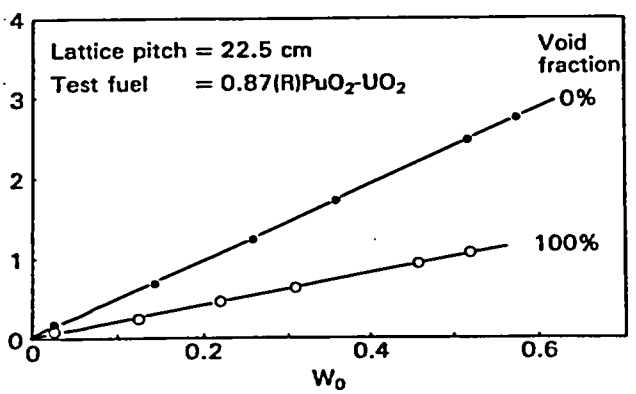

Fig. 5. Change in critical axial buckling as a function of statistical weight for two different void fractions.

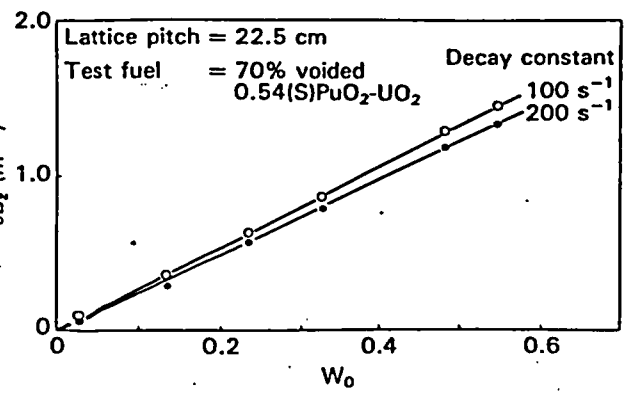

Fig. 6. Change in geometric axial buckling as a function of statistical weight for two fixed values of decay constants.

fraction as compared with that of 1.2 UO_2 fuel. The B_m^2 values of the two kinds of 0.87 PuO_2-UO_2 fuel have differences of 18 to 26% according to the range of void fraction.

In the data analysis of the experiment, the dependence of B_m^2 of a test lattice on the maximum number of substituted clusters N_{max} was examined. An example of the change of B_m^2 obtained by changing N_{max} is shown in Fig. 7. If N_{max} is 5, B_m^2 reaches a constant value within <1% at most. This means that the coolant void reactivity of the test lattice can be determined with an accuracy of ~10%, regardless of the kinds of test fuel, by substituting ~5% of the total number of charged clusters.

To examine the propriety of applying the first-order perturbation theory, B_m^2 of the test lattice was compared with B_m^2 determined according to the second-order perturbation theory[13] under the same lattice condition. As a result, B_m^2 of each test lattice determined from the present experiment agreed with B_m^2 of the former experiment within ±3% on the average. Therefore, the present method was sufficiently applied to the data analysis for the substitution measurement on HWR lattices.

The experimental results of void reactivity in test lattices are shown in Table VI in comparison with reference lattices. When a large change was given to the void fraction (i.e., 0 to 100%), the void reactivity in the small DCA core became a large negative value due to the larger leakage effect. The effect that fuel composition exerts on void reactivity was examined. It was determined in comparison with the void reactivity of both lattices having 1.2 UO_2 fuel and 0.54(S) PuO_2-UO_2 fuel that plutonium largely shifted the void reactivity toward the negative side more than the uranium did. Also, from the comparison of the void reactivity

TABLE V

Experimental Value of Material Buckling

Lattice Pitch (cm)	Fuel Kind	Void Fraction (%)	Material Buckling (m^{-2})	
			B_z^2	B_m^2
22.5	1.2 UO_2	0	8.59 ± 0.18	11.07 ± 0.18
		30	8.49 ± 0.17	10.96 ± 0.17
		70	7.77 ± 0.15	10.24 ± 0.15
		87	7.66 ± 0.15	10.13 ± 0.15
		100	6.47 ± 0.11	8.83 ± 0.11
	0.54(S) PuO_2-UO_2	0	12.87 ± 0.32	15.34 ± 0.33
		30	12.04 ± 0.30	14.51 ± 0.30
		70	10.48 ± 0.24	12.95 ± 0.24
		87	9.96 ± 0.23	12.43 ± 0.23
		100	8.49 ± 0.18	10.85 ± 0.18
	0.87(S) PuO_2-UO_2	0	18.95 ± 0.65	21.42 ± 0.66
		100	10.86 ± 0.26	13.23 ± 0.26
	0.87(R) PuO_2-UO_2	0	13.27 ± 0.35	15.74 ± 0.35
		100	8.43 ± 0.17	10.79 ± 0.17
25.0	1.2 UO_2	0	7.27 ± 0.14	9.71 ± 0.14
		100	7.25 ± 0.14	9.56 ± 0.14
	0.54(S) PuO_2-UO_2	0	10.86 ± 0.25	13.30 ± 0.26
		100	9.35 ± 0.20	11.66 ± 0.20
	0.87(S) PuO_2-UO_2	0	15.79 ± 0.47	18.24 ± 0.47
		100	12.05 ± 0.29	14.36 ± 0.29

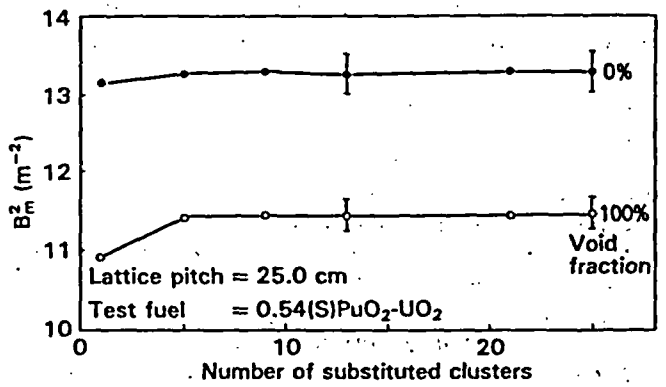

Fig. 7. Converged material buckling of test lattice as a function of substituted clusters for two different void fractions.

of two kinds of 0.87 PuO_2-UO_2 fuel, it was found that the shift of the void reactivity toward the negative side was more conspicuous as the content of fissile plutonium increased.

The void reactivity is shown in Fig. 8 for both lattices having 1.2 UO_2 fuel and 0.54(S) PuO_2-UO_2 fuel when void fraction was changed from 0 through 30, 70, and 87% to 100%, respectively. The void reac-

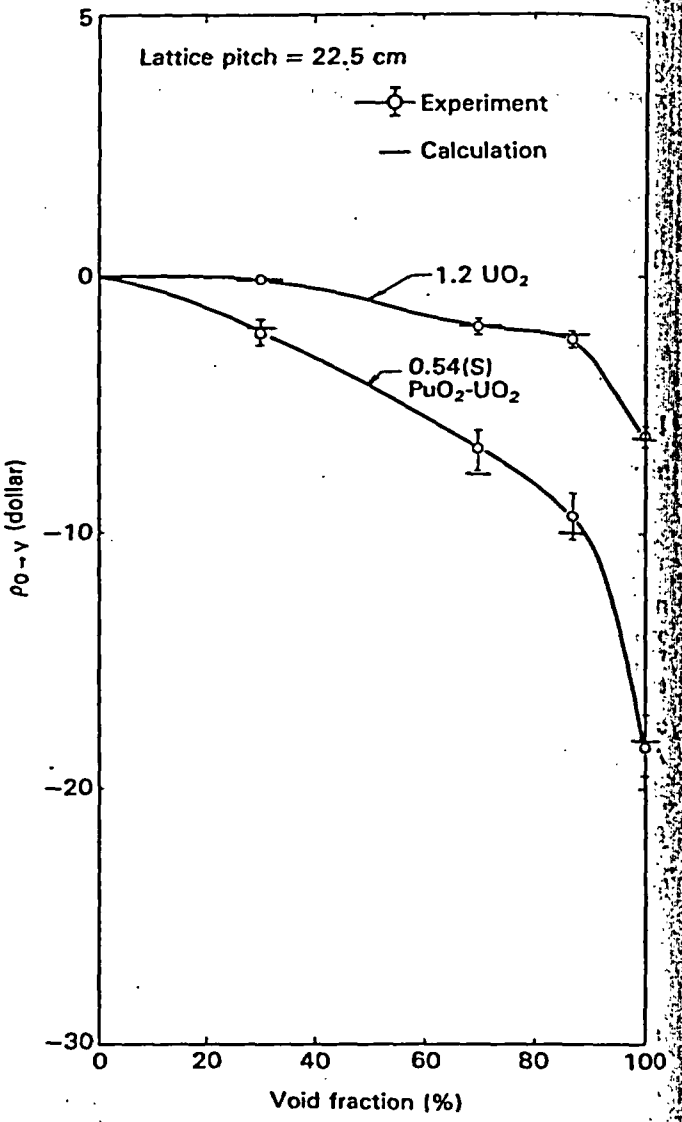

Fig. 8. Void reactivity due to change in coolant void fraction from 0%.

tivity shifted gradually toward the negative side as the void fraction increased, and it rapidly lowered to a large negative value when the void fraction was close to 100%. This occurred because the microscopic scattering cross section of thermal neutrons for light water was as large as ~100 b. The atomic number density of light water, however, became zero in the case of 100% void fraction; therefore, the diffusion coefficient rapidly increased. When the void fraction became 100%, the increase of neutron leakage $\delta D_z \cdot B_z^2$ due to a large axial buckling and the decrease of moderating effect contributed more to the reactivity than the decrease of the absorption effect of light water.

The dependence of void reactivity on fuel composition was examined. Here, the macroscopic absorption cross section Σ_a^{2200} of fuel for thermal neutrons

TABLE VI

Comparison Between Experiment and Calculation for Coolant Void Reactivity

Lattice Pitch (cm)	Fuel Kind	Change in Void Fraction (%)	Void Reactivity (dollar)	
			Experiment	Calculation
22.5	1.2 UO_2	0 → 30	−0.22 ± 0.06	−0.16
		0 → 70	−2.01 ± 0.26	−2.00
		0 → 87	−2.51 ± 0.31	−2.32
		0 → 100	−6.31 ± 0.43	−6.31
		30 → 70	−1.74 ± 0.25	−1.81
		30 → 87	−2.22 ± 0.29	−2.12
		30 → 100	−6.00 ± 0.41	−6.06
		70 → 87	−0.30 ± 0.09	−0.15
		70 → 100	−3.96 ± 0.33	−3.72
		87 → 100	−3.64 ± 0.32	−3.54
22.5	0.54(S) PuO_2-UO_2	0 → 30	−2.24 ± 0.54	−2.02
		0 → 70	−6.81 ± 0.75	−7.84
		0 → 87	−9.36 ± 0.88	−10.17
		0 → 100	−18.39 ± 1.30	−18.28
		30 → 70	−4.49 ± 0.63	−5.47
		30 → 87	−6.79 ± 0.76	−7.60
		30 → 100	−15.09 ± 1.14	−15.24
		70 → 87	−1.74 ± 0.46	−1.67
		70 → 100	−8.63 ± 0.86	−8.21
		87 → 100	−6.42 ± 0.76	−6.24
	0.87(R) PuO_2-UO_2	0 → 100	−19.30 ± 1.30	−20.87
	0.87(S) PuO_2-UO_2		−28.30 ± 2.08	−29.89
25.0	1.2 UO_2	0 → 100	−0.06 ± 0.02	+0.20
	0.54(S) PuO_2-UO_2		−5.89 ± 0.77	−6.33
	0.87(S) PuO_2-UO_2		−14.21 ± 1.46	−14.31

of 2200 m/s was used as a variable representing the difference of fuel. The relation of Σ_a^{2200} to the void reactivity $\rho_{0\to100}$ when void fraction was changed from 0 to 100% was clarified. The microscopic absorption cross sections of fuel substances were used from the values of Ref. 19, and the atomic number densities of respective elements were used from the inspection data. The relation between $\rho_{0\to100}$ and Σ_a^{2200} is shown in Fig. 9 using lattice pitch as a parameter. As seen in this figure, the increase of Σ_a^{2200} moved $\rho_{0\to100}$ toward the negative side regardless of lattice pitch. Since the width of change of Σ_a^{2200} (corresponding to the degree of enrichment of plutonium) used for the experiment was ~30% (0.25 to 0.35 cm^{-1}) at most, $\rho_{0\to100}$ of the lattices having two kinds of PuO_2-UO_2 fuel (enrichment 0.54 and 0.87%) was regarded as monotonously changing. Straight lines connected $\rho_{0\to100}$ of 0.54(S) and 0.87(S) PuO_2-UO_2 fuel lattices every lattice pitch. In Fig. 9 two points are clarified:

1. The increases of Σ_a^{2200} shifted $\rho_{0\to100}$ toward the negative side.

2. Even in the fuel of the same Σ_a^{2200}, $\rho_{0\to100}$ became more negative as lattice pitch was narrower.

It is also clear that $\rho_{0\to100}$ for 0.87(R) PuO_2-UO_2 fuel is situated above the continuous line, and that if the continuous line is directly extrapolated up to Σ_a^{2200} corresponding to 1.2 UO_2 fuel, $\rho_{0\to100}$ for the 1.2 UO_2 fuel in every lattice pitch is situated above each extrapolated line. Therefore, two more points are clarified:

3. In the PuO_2-UO_2 fuel of the same degree of enrichment of plutonium, $\rho_{0\to100}$ shifted farther to the

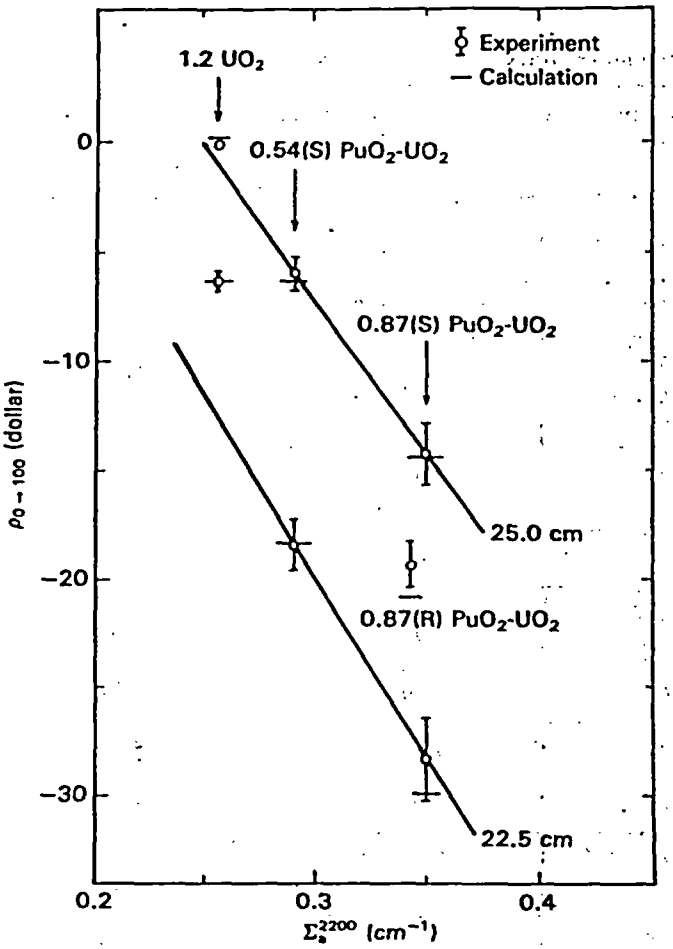

Fig. 9. Dependence of 0 → 100% void reactivity on 2200 m/s absorption cross section of fuel.

negative side as the proportion of fissile plutonium increased.

4. In the fuel of the same Σ_a^{2200}, PuO_2-UO_2 fuel shifted $\rho_{0\to100}$ even farther to the negative side than UO_2 fuel.

We examined the fuel composition dependence of void reactivity from the lattice characteristics viewpoint. The increase of Σ_a^{2200} shifted $\rho_{0\to100}$ toward the negative side mainly because of the thermal neutron utilization, which increased because the increase in void fractions became smaller in the fuel with larger Σ_a^{2200}. This is clear because the relative absorption effect of coolant became smaller with large Σ_a^{2200}.

Item 2 can be explained as follows. If lattice pitch is wide, the relative moderator-to-fuel volume ratio V_m/V_f is large (for 22.5-cm pitch, $V_m/V_f = 7.5$; for 25.0-cm pitch, $V_m/V_f = 10.0$), and neutrons are sufficiently thermalized. Therefore, it was difficult to affect neutron spectra with coolant. Plutonium was more effective for reducing void reactivity than uranium in a narrower pitch lattice. This fact can be examined by comparing the change of the resonance reaction rate of plutonium and uranium near 0.3 eV due to the change of void fraction. The degree of neutron spectra hardening due to the increase of void fraction was more conspicuous as lattice pitch became narrower. In particular, since resonance exists in plutonium, when lattice pitch was narrow, the spectra were more hardened in a PuO_2-UO_2 fuel lattice as compared with a UO_2 fuel lattice.[20,21] However, when lattice pitch became wide, the degree of spectrum hardening due to the increase of void fraction was not much different according to the difference of fuel substances such as uranium and plutonium. As a result, the difference between UO_2 and PuO_2-UO_2 fuels regarding the change of resonance reaction rate due to the increase of void fraction increased as lattice pitch was narrower. So the void reactivity was more negative in the PuO_2-UO_2 fuel than in the UO_2 fuel.

For items 3 and 4, since plutonium has resonance in a low energy region (0.3 to 1.0 eV) unlike uranium, $\rho_{0\to100}$ differed according to the nuclides of fuel substances. The neutron spectra in fuel clusters tended to harden as void fraction became higher, but this tendency was more conspicuous in plutonium than in uranium having a cross section of nearly $1/v$; the macroscopic absorption cross sections of resonance energy near 0.3 and 1.0 eV of plutonium became larger as void fraction increased, but the increase of the cross sections became larger as the plutonium content in fuel increased. As a result, when void fraction increased, the macroscopic absorption cross section near the resonance energy became larger. Inversely, the neutron flux there tended to be depleted; therefore, the effect that the change of resonance absorption rate exerted on void reactivity decreased as the plutonium content increased. If void fraction was high, the neutron flux in the resonance energy region in a pressure tube tended to be depleted because the slowing down effect due to light water was large if void fraction was low. Therefore, the neutron flux in the resonance energy region recovered the amount decreased by resonance absorption. Its recovering effect, however, decreased as void fraction became higher; the neutron flux tended to be depleted. Consequently, in the PuO_2-UO_2 fuel containing such fissile substances as ^{239}Pu and ^{241}Pu having a very large resonance near 0.3 eV (total cross section = ~5000 and 2000 b, respectively), the decrease of resonance fission rate due to the increase of void fraction contributed to this effect. On the other hand, the decrease of resonance capture rate contributed in the fuel having large amounts of ^{240}Pu and ^{242}Pu. However, since the total resonance cross section near 1.0 eV of ^{240}Pu and ^{242}Pu is as large as several tens of thousands of barns, the neutron flux in the resonance region was more depleted in the fuel containing these nonfissile substances. The neutron flux near the resonance region was sufficiently small compared with that

in a Maxwellian region. Accordingly, the effect that the resonance of ^{240}Pu and ^{242}Pu exerted on void reactivity can be neglected. Although the ^{240}Pu and ^{242}Pu content of 0.54(S) PuO_2-UO_2 fuel largely differs from that of 0.87(R) PuO_2-UO_2, void reactivities are nearly the same between these two fuel lattices, as shown in Fig. 9. Resonance of ^{239}Pu is the most dominant effect on void reactivity in plutonium nuclides.

IV.B. Comparison of Experimental and Calculated Values

The experimental void reactivities were the values for single fuel lattices, so that those can be compared directly with the values by lattice calculation. The calculated values by the lattice calculation code[22] WIMS-D were compared with the experimental ones. The WIMS-D code is used for the nuclear design of commercial HWRs in Japan. The code is based on the transport theory, and the basic cross-section library is 69 groups. The collision probability method has been adopted for solving a transport equation. This method has confirmed the accuracy in the critical experiment using DCA. The neutron energy group on the calculation is 7 groups in the thermal region, and 11 groups in resonance and fast regions, 18 groups total. The R-θ geometry was adopted, and the number of meshes was 42 in the radial direction and 12 in the azimuthal direction. Neutron leakage in the finite system was evaluated by B_1 approximation. For treating the anisotropy of neutron diffusion in axial and radial direction due to the heterogeneity of lattices, the diffusion coefficient determined by Benoist's method[23,24] was taken into account.

The calculated and experimental values are shown in Table V. Since the experimental core was small, the contribution of the axial neutron leakage to void reactivity was considerably large. In addition, HWR lattices had a strong heterogeneity, and an ~5% anisotropy arose in the neutron diffusion coefficient according to the calculation. If the anisotropy of the diffusion coefficient was introduced, the difference between the experimental and calculated values tended to be small.

Experimental and calculated values for 1.2 UO_2 fuel lattices agreed well in whatever void fraction change, and the difference was within ±0.3 dollar. The disagreement between both values for the 0.54(S) PuO_2-UO_2 fuel lattice was within ±0.3 dollar if the width of void fraction change was small. However, if the change of void fraction was large, the discrepancy became ±1.0 dollar. With the increase of enriched plutonium or the absolute values of void reactivity, the calculated values approximately tended to underestimate in comparison with experimental values, and the discrepancy was ~1.6 dollar at maximum.

Heterogeneity increased with increasing lattice pitch. Then, reducing the accuracy of calculation was predicted, but the accuracy had no meaningful dependence on the lattice pitch when fuel composition was the same. If the fuel enrichment increased, the critical volume decreased and the leakage effect to the void reactivity became overwhelmingly large. The accuracy of calculation of the diffusion coefficient was the main factor affecting the accuracy of calculation of void reactivity, because the neutron flux distribution was a simple shape and the change of void fraction was large.

V. CONCLUSION

By applying the first-order perturbation theory to the analysis of the experimental data of the substitution method including the pulsed neutron method, the coolant void reactivity of the test lattice could be determined, even if only a small number of fuels can be prepared. Three kinds of PuO_2-UO_2 fuel were used as test fuels, and 1.2% enriched UO_2 fuel was used as the reference.

In the analysis of the experimental data, three assumptions were introduced:

1. Both reference and test lattices are homogeneous.
2. Diffusion approximation can be applied.
3. The differences of diffusion coefficient and neutron velocity between a reference lattice and a test lattice can be neglected.

The relation between the statistical weight of the substituted region and the amount of change in the axial buckling due to substitution was expressed by a linear equation having the gradient peculiar to a test lattice. When the minimum number of the fuel clusters for substitution was ~5% of the total ones, the coolant void reactivities of test lattices were determined with an accuracy of ~10%.

By this substitution measurement, the dependence of void reactivity on fuel substances, the isotopic ratio of plutonium, and lattice pitch in HWRs was clarified from the viewpoint of the effect of neutron spectra and the change of resonance absorption rate near 0.3 eV. Also, it was clarified that the lattice calculation code WIMS-D could be evaluated by the void reactivity of about −30 dollar in maximum within 1.6 dollar.

ACKNOWLEDGMENTS

We are indebted to K. Shiba and M. Muramatsu for their helpful cooperation in measurements. We are also grateful to Y. Miyawaki and K. Iijima for fruitful advice.

We wish to thank the staff members of the Heavy Water Critical Experiment Section Oarai, Power Reactor and Nuclear Fuel Development Corporation, for their support in this series of experiments.

REFERENCES

1. H. KATO and Y. MIYAWAKI, *Trans. Am. Nucl. Soc.*, 23, 513 (1976).

2. S. SHIMA and S. SAWAI, "The FUGEN Project," *Proc. Canadian Nuclear Association Annual Conf.*, Ottawa, Ontario, Canada, June 11-14, 1972, p. 204, Canadian Nuclear Association (1973).

3. W. E. GRAVES, "Analysis of the Substitution Technique for the Determination of D_2O Lattice Bucklings," DP-832, Savannah River Laboratory (1963).

4. H. R. LUTZ, T. AUERBACH, W. HEER, and R. W. MEIER, *IAEA Bull.*, 2, 85 (1964).

5. D. C. KING and M. GIBSON, "An Analysis of Some Two-Zone Exponential Experiments on Graphite Moderated Lattices," AEEW-R428, U.K. Atomic Energy Authority, Winfrith (1965).

6. G. BLAESSER, *IAEA Bull.*, 3, 443 (1964).

7. D. S CRAIG, R. E. GREEN, and A. OKAZAKI, *Trans. Am. Nucl. Soc.*, 9, 126 (1966).

8. R. PERSSON, *IAEA Bull.*, 3, 289 (1964).

9. W. B. ROGERS, V. D. VANDERVELDE, and N. P. BAUMANN, *Trans. Am. Nucl. Soc.*, 8, 449 (1965).

10. R. PERSSON, "One-Group Perturbation Theory Applied to Substitution Measurements with Void," AE-248, AB Atomenergi, Sweden (1966).

11. R. PERSSON, *Nukleonik*, 10, 163 (1967).

12. G. CASINI and J. MEGIER, *IAEA Bull.*, 3, 423 (1964).

13. K. SHIBA, *Nucl. Sci. Eng.*, 65, 492 (1978).

14. S. GLASSTONE and M. C. EDLUND, *The Elements of Nuclear Reactor Theory*, D. Van Nostrand Company, New York (1952).

15. B. E. SIMMONS and J. S. KING, *Nucl. Sci. Eng.*, 3, 595 (1958).

16. F. AMANO, *J. Nucl. Sci. Technol.*, 6, *12*, 689 (1969).

17. A. ALPIAR, "METHUSELAH I, A Universal Assessment Programme for Liquid Moderated Reactor Cells Using IBM 7090 or STRETCH Computer," AEEW-R135, U.K. Atomic Energy Authority, Winfrith (1963).

18. T. B. FOWLER, D. R. VONDY, and G. W. CUNNINGHAM, "Nuclear Reactor Core Analysis Code: CITATION," TM-2496, Revision 2, Oak Ridge National Laboratory (1971).

19. D. J. HUGHES and R. B. SCHWARTZ, "Neutron Cross Sections," BNL-325, 2nd ed., Brookhaven National Laboratory (1958).

20. N. FUKUMURA, *J. Nucl. Sci. Technol.*, 4, *18*, 45 (1981).

21. P. M. FRENCH, "Detailed Neutron Activation Measurements in Lattices with 31-Element PuO_2-UO_2 Clusters of Simulated Burned-Up Natural Uranium Fuel in Heavy Water Moderator," AECL-7908, p. 103, Atomic Energy of Canada Ltd., Chalk River (1983).

22. J. R. ASKEW, F. J. DAYERS, and P. B. KEMSHELL, *J. Brit. Nucl. Soc.*, 5, 564 (1966).

23. P. BENOIST, *At. Energy Res. Establ., Transl.*, 842 (1959).

24. P. BENOIST, *At. Energy Establ. Winfrith, Transl.*, 4 (1962).